vehicles

MDPI

Article

Evolution of the Hybrid Aerial Underwater Robotic System (HAUCS) for Aquaculture: Sensor Payload and Extension Development

Casey J. Den Ouden [1,*], Paul S. Wills [1], Lucas Lopes [1], Joshua Sanderson [2] and Bing Ouyang [1]

[1] Systems and Imaging Laboratory (SAIL), Harbor Branch Oceanic Institute, Florida Atlantic University, 5600 US 1 North, Fort Pierce, FL 34946, USA; pwills2@fau.edu (P.S.W.); lucaslopez2016@fau.edu (L.L.); bouyang@fau.edu (B.O.)

[2] Harriet L. Wilkes Honors College, John D. MacArthur, Florida Atlantic University, 5353 Parkside Dr, Jupiter, FL 33458, USA; jsanderson2020@fau.edu

* Correspondence: cdenouden@fau.edu

Abstract: While robotics have been widely used in many agricultural practices such as harvesting, seeding, cattle monitoring, etc., aquaculture farming is an important, fast-growing sector of agriculture that has not seen significant adoption of advanced technologies such as robotics and the Internet of Things (IoT). In particular, dissolved oxygen (DO) monitoring, a practice in pond aquaculture essential to the health of the fish crops, remains labor-intensive and time-consuming. The Hybrid Aerial Underwater robotiCs System (HAUCS) is an IoT framework that aims to bring transformative changes to pond aquaculture. This paper focuses on the latest development in the HAUCS mobile sensing platform and field deployment. To address some shortcomings with the current implementation, the development of a novel rigid Kirigami-based robotic extension subsystem that can expand the functionality of the HAUCS platform is also being discussed.

Keywords: field robotics; hybrid sensing platform; aquaculture; HAUCS; Internet of Things; origami; robotic extension; mobile agent; LoRa

check for updates

Citation: Den Ouden, C.J.; Wills, P.S.; Lopes, L.; Sanderson, J.; Ouyang, B. Evolution of the Hybrid Aerial Underwater Robotic System (HAUCS) for Aquaculture: Sensor Payload and Extension Development. *Vehicles* **2022**, *4*, 390–408. https://doi.org/10.3390/vehicles4020023

Academic Editors: Ralf Stetter, Udo Pulm, Markus Till and Giulio Reina

Received: 22 February 2022
Accepted: 15 April 2022
Published: 21 April 2022

Publisher's Note: MDPI stays neutral with regard to jurisdictional claims in published maps and institutional affiliations.

Copyright: © 2022 by the authors. Licensee MDPI, Basel, Switzerland. This article is an open access article distributed under the terms and conditions of the Creative Commons Attribution (CC BY) license (https://creativecommons.org/licenses/by/4.0/).

1. Introduction and Background

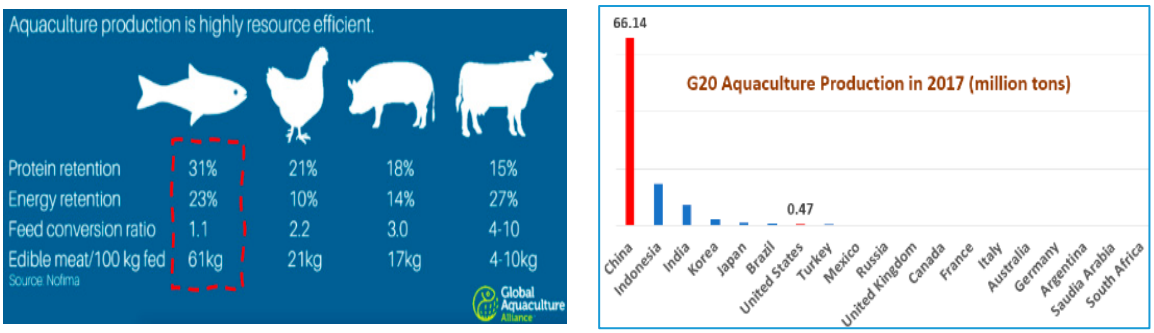
Challenges in Aquaculture Farming

Precision agriculture (PA) combines robotic field machines and information technology in agriculture and plays an increasingly important role in farm production. PA-related advanced technologies such as the Internet of things (IoT), robotics, and artificial intelligence (AI) have been an active research topic and have seen robust growth [1–3]. Importantly, research results in CPS have been successfully adopted in many agriculture industry sectors. A BI Intelligence survey expects the adoption of IoT devices in the agriculture industry to reach 75 million in 2020, growing 20% annually [4]. In addition, the global smart agriculture market size is expected to triple by 2025, growing from 5 billion USD in 2016 to over 15 billion USD [4].

However, a critical agriculture sector that has been left behind is aquaculture. Aquaculture is farming in an aquatic environment. As an agricultural practice, aquaculture is characterized by considerable diversity in habitats, methods, and species. The species range from "livestock" (e.g., fish, mollusks, and crustaceans) to plants (e.g., microalgae, macroalgae, and vascular plants). The systems employed include earthen ponds, tanks, or open water (nearshore or offshore), depending on the habitat where production occurs. Pond and tank systems are generally land-based, and net pens or bottom cultures are in open water. Underpinning all of these are the energy systems powering the farm operations.

Worldwide aquaculture plays an essential role in food security in the seafood sector, filling the need and demand gap due to stagnant capture fisheries output. The transition

from fisheries to aquaculture has been growing at an average rate of >6% annually. Since 2014, more farmed seafood than wild-caught seafood has been consumed globally, with more than half of all seafood coming from farms [5]. It is also important to emphasize that compared with other farmed proteins (e.g., chicken and beef), seafood has the highest resource efficiency, lowest feed conversion ratio (i.e., most efficient in converting feed to animal proteins) (Figure 1a), aquaculture produces lower greenhouse gas emissions than other types of farming [6]. Farmed fish are less resource-intensive overall than other common animal-based protein products and consume less water for production than pork and beef in many cases [7,8]



(**a**) (**b**)

Figure 1. (**a**) The high resource efficiency of fish compared with other farmed proteins [6]; (**b**) aquaculture production in 2017 among the G20 countries. China (66.14 Mts) and the US (0.47 Mts) are highlighted in red [9].

Management of water quality, particularly dissolved oxygen (DO), is critically important for successful operation in aquaculture fish farming. DO depletion is a leading cause of fish mortality on farms [10]. Catastrophic loss can occur within hours if ponds are not appropriately managed. The current management practice on pond-based farms uses human operators who drive trucks or other all-terrain vehicles throughout the day, especially at night, to sample and monitor the DO in each pond (Figure 2a). The associated labor and equipment costs limit the scope and frequency of such sampling since each sensor-equipped truck must manage dozens of ponds. To obtain the required monitoring frequency for proper management, large farms require multiple drivers and sampling instruments. The level of resolution that this approach can achieve on any pond is generally restricted to a single nearshore measurement at a point on the pond with a well-maintained roadbed. On large ponds (e.g., 2 to 8 hectares), this may result in a failure to promptly identify localized water quality problems that can ultimately affect a large percentage of the stock. Even though readings should be taken hourly on each pond, large farms (>400 hectares) with hundreds of ponds may only be outfitted to take readings at much lower frequencies due to the high labor and equipment costs of operating large fleets of monitoring vehicles. Measurements of additional water quality parameters cannot be performed due to the demanding schedules required of drivers to achieve the minimum frequency for DO management. The current monitoring practice relies on human operators to drive a truck around the farm to measure the DO concentration in each pond. An example of a typical DO measurement truck is shown in Figure 2a. Such practice has deficiency on multiple fronts: (1) human data collection may be difficult to interpret or recorded incorrectly; (2) the sensor is mounted onto a boom that is operated from within the cab of the vehicle, meaning the operator is unaware if they breach the air/water interface for acceptable readings to occur; (3) weather variability may cause the water levels of the ponds to decrease, this prevents the operators from receiving acceptable data as the sensor may not even reach the current water level and (4) fuel cost may become prohibitively high on large farms that may require a few dozen of such trucks. Furthermore, with the current practice, operators have a very limited window of time (e.g., less than an hour in

the middle of the night) to react to potential oxygen depletion, increasing the likelihood of catastrophic events. The response (e.g., putting emergency aeration equipment in a pond) takes time away from achieving DO measurement frequencies.



Figure 2. (**a**) The typical truck-based boom senor system. (**b**) The "top-of-the-line" in situ buoy system from In-Situ Inc [11].

The industry has attempted to remedy the deficits of present truck-based aquaculture monitoring through in situ pond buoy monitoring systems (Figure 2b) [11]. However, these platforms are a temporary fix as they suffer negative attributes. In an aquaculture farm system, there is always a plethora of bacteria and other organics in the ponds. This will inevitably result in biofouling. Since the aquaculture ponds are generally very productive, the growth of organic material such as algae, Bivalvia, etc., on a sensor surface due to biofouling would quickly render the platform useless.

Similarly, maintenance on these platforms is labor-intensive. It requires a laborer to enter the pond to retrieve the device or an elaborate pully system that would cause stress to the stock within the pond. The farm technicians need to remove the sensor suite from the pond before starting stock extraction when harvesting. Many farms have employed the buoy-based systems and subsequently abandoned them due to long-term difficulties in application.

The Hybrid Aerial/Underwater robotiC System (HAUCS) framework aims to mitigate the aforementioned issues to provide automated, high-density monitoring of key environmental metrics of each aquaculture pond on a farm using relatively inexpensive robotic sensing platforms.

A critical aspect of the HAUCS sensing platform is a novel deployable robotic extension. This subsystem is essential to reduce the drag of the HAUCS platform during the flight and improve the platform stability during the sensing operation. Stability during sensing is even more critical to expand our sensor payload beyond DO monitoring to include underwater cameras or sonars to support other farm operations.

This design relies on Origami principles to realize rigid structures that retain their shape even under transverse loading. We will therefore provide a brief discussion on Origami. Origami is the ancient art of folding, generally, the word conjures images of intricate paper structures [12,13]. Origami has been adopted for many engineering applications where a package with limited initial storage space is required to morph into a structure with a significantly larger span. This is accomplished by employing the governing geometric calculations at the heart of Origami to create more complex structures. One of the well-known applications is the NASA Solar Panel Array [14]. Additional applications include circuit board design [15], shelters [16], and biomedical devices [17]. Peraza-Hernandez et al. provide an excellent review in [18].

At the fundamental level, the deployable robotic extension under consideration is a cylindrical tube that can be folded in the axial direction to a flat state on demand. One Origami pattern of interest is the twist buckling pattern or the Kresling Origami pattern [19–22], formed by the buckling of a thin cylindrical shell under torsional loading. The properties of the Kresling pattern have been studied extensively [23–26].

In particular, the Kresling pattern is preferable to the axially loaded Yoshimura or diamond origami [26] in that the Yoshimura pattern is not continuously foldable, and significant stretching occurs during the re-stabilization stage [24]. The Kresling pattern was demonstrated experimentally in [24]. In the experiments, a thin-walled sheet is wrapped around two coaxial mandrels. When the mandrels are twisted, a highly regular self-organized folding pattern appears across the gap, formed by inclined and elongated parallelograms (mountain-folds), divided on their long diagonal by a valley-fold [24,27].

Origami-based deployable robotic extension for drones has been previously studied by Kim et al. [28]. The extension is designed to "fold-flat" whilst flying and deploy into the rigid structure while hovering at a given point. The end effector was designed to be plug-and-play so they could easily switch between a gripper mechanism and a camera. In their design, the axially loaded Origami pattern was adopted. In this regard, the pattern can be considered a variant of the Yoshimura Origami. The folding and unfolding are achieved via an indirect tendon system—a wire runs the length of the structure and is controlled by a motor attached to the drone body. The team designed a locker system to counteract transverse force loadings on the expanded structure. These lockers are moved in conjunction with the wire deployment and retraction. Additionally, they are strengthened with magnets.

In the context of the HAUCS platform, there are several deficiencies in the aforementioned approach. The first constraint in utilizing this design is the mechanical restrictions. The structure must fully expand or retract as the system is operated by indirect force. The arm cannot be halted partway through the deployment or retrieval. This is intrinsic to the Yoshimura Origami [29].

Additionally, due to the complexity of the locker system, while the design succeeds in its objective of rigidity, it severely limits the flexibility of the robotic extension. As such, the current design will not be able to achieve more complex configurations. Thirdly, the folded footprint will be twice as large, which may not be desirable for field robots in aquaculture applications.

With the main focus of our current endeavors being to realize the HAUCS framework, the paper structure is as follows. In Section 2, we review the HAUCS concept and previous development efforts. Section 3 presents our current sensor, platform development, and field experimental results. We discuss our effort to develop a versatile robotic extension in Sections 4 and 5 and conclude in Section 6.

2. Overview of the HAUCS Framework

The overarching goal of HAUCS is to relieve human operators from the most labor-intensive, time-consuming, and expensive tasks in aquaculture farming operations through a group of cooperative robotic sensing and actuator platforms. With support from the National Institute of Food and Agriculture (NIFA), USDA, through the Ubiquitous Collaborative Robots (NRI-2.0) program, the project was launched in the Spring of 2019.

HAUCS is a framework that aims to achieve collaborative monitoring and decision-making on aquaculture farms of varying scales. The HAUCS framework consists of three basic modules: aero-amphibious robotic sensing platforms integrated with underwater sensors, land-based infrastructure, and backend modeling and processing infrastructure, particularly an ML-based water quality prediction model. Each HAUCS autonomous unmanned platform (AUP) consists of an unmanned robotic vehicle and submerged underwater sensors. Data from the underwater sensors attached to the AUP, such as DO and temperature sensors, will be sent to the farm control center via a radio link during sensing operations. Sensor data from all the ponds on the farm and the associated weather data will be used to train an ML-based prediction model. The model prediction can, in turn, guide other instruments to mitigate an emergency situation (e.g., turning on a fixed aerator or instructing human operators to move mobile emergency aeration equipment into place in a pond). The overall concept of operations is illustrated in Figure 3 [30].

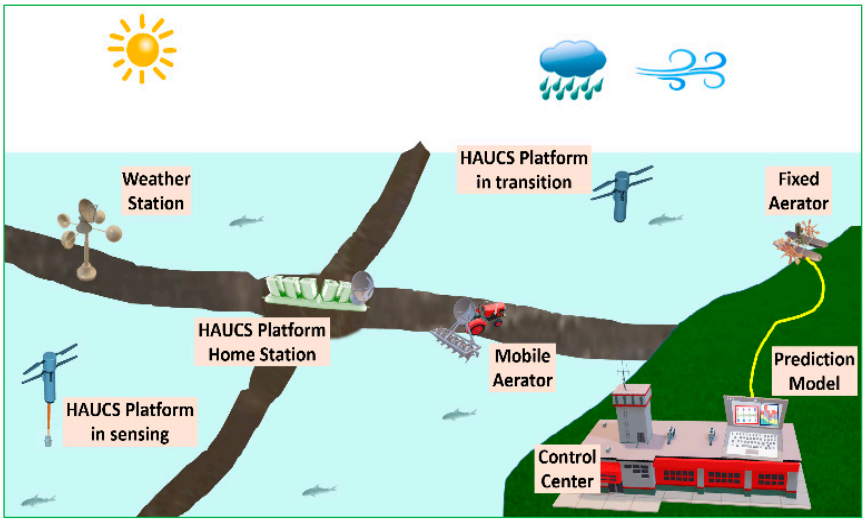


Figure 3. A basic HAUCS concept of operations [30].

The agility of the HAUCS platform supports a level of precision that is unobtainable by the truck-based monitoring systems. The HAUCS platform expands the sampling capabilities by allowing the farmers to sample multiple points within a pond. In contrast, truck-based monitoring is limited to a single-point sampling near the edge of the pond. Various novel sensing schemes can be investigated to optimize spatial and temporal regions being studied by utilizing the platform's mobility. One potential sampling scheme sees the platform enter a new pond where the platform will hover for approximately 30 s so the DO sensor can record an accurate reading. The platform will then move through the pond toward a neighboring pond, the sensor maintaining its submergence below the water surface to collect a stream of water quality data (Figure 4). Through sampling routes such as this, it acquires significantly more data samples and captures the spatial variability of water quality in any given pond.

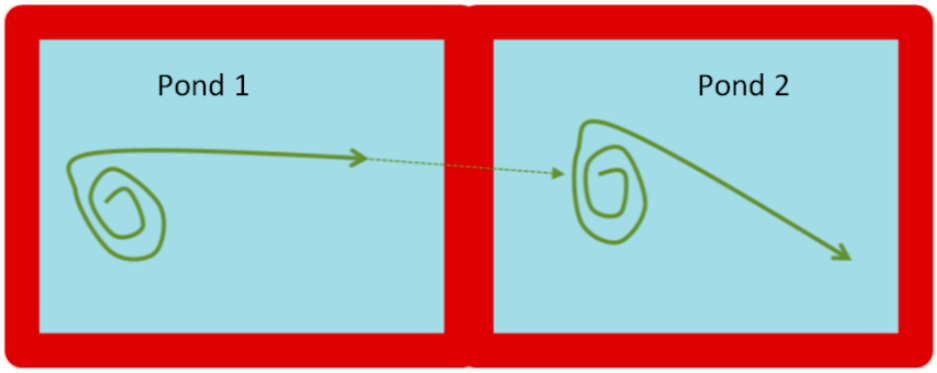


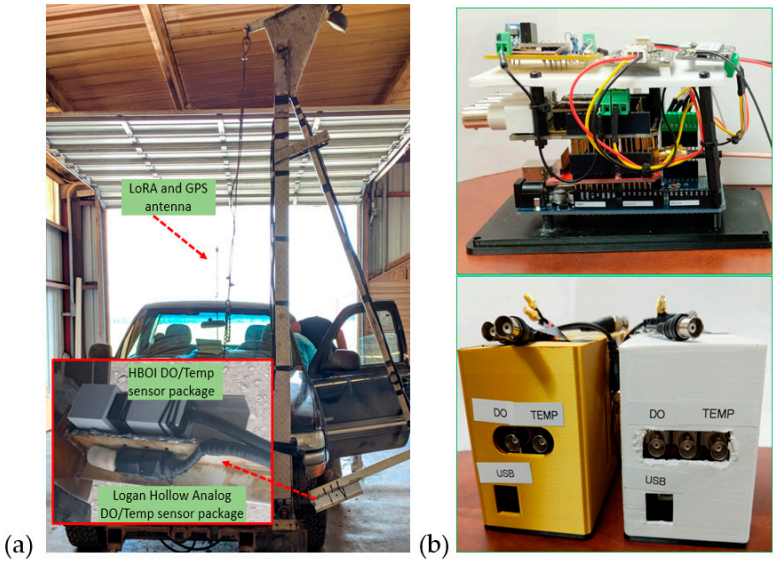
Figure 4. Illustration of the mobile platform-based sensing [30].

This highly scalable framework will convert aquaculture farm operations to an "Internet of Aquaculture." In particular, the DO sensing platform will transition from a truck-based manual measurement practice to an intelligent, automated scheme relying on aerial drones integrated with underwater sensors. Compared with the state-of-the-art solutions, the advantages of HAUCS include:

- Improved scalability—compared with the sensor buoys, HAUCS design can be easily adapted to farms of varying scales.
- Broad spatial coverage—capable of realizing novel sensing patterns to cover different areas on a large pond, hence providing more accurate reporting of pond conditions.
- Mitigated biofouling—avoiding sensors in bio-productive water.

- Supporting novel sensing schemes to cover extended spatial regions and generate more robust readings than the traditional truck-based data acquisition.

A stop-gap truck-based automated sensor system was developed for three reasons: (1) to provide an automated DO data acquisition system compatible with the current monitoring practice on the farm that will transition seamlessly to the drone-based platform; (2) to evaluate the infrastructure need for future deployment of HAUCS platforms on the farm, and (3) to collect high-quality data to support prediction model development. This prototype sensor system consists of a mobile data acquisition system (DAQ) and a central server. The mobile DAQ was installed on the farm sensing truck, side by side with the DO sensor used in the farm operation at the Logan Hollow Fish Farm (Figure 5a). The central server was located inside the farm manager's office.



(a) (b)

Figure 5. DO sensing truck with HBOI sensor head co-mounted with the original DO sensor. (**a**) HBOI sensors mounted side-by-side with Logan Hollow sensors. (**b**) In-truck control unit.

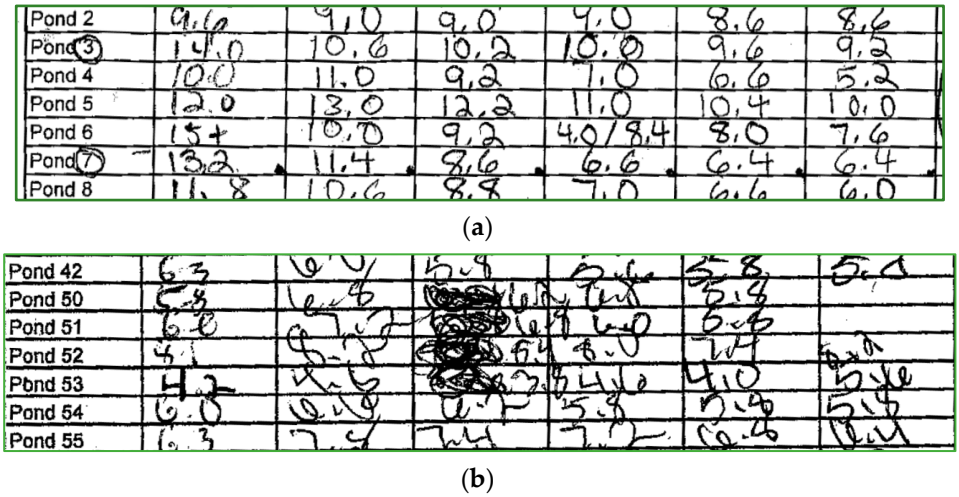
As shown in Figure 5b, the sensor control system is an Arduino Mega integrated with Atlas Scientific™ temperature and DO shields to simplify the integration of the sensor with the backend controller. In addition to the sensor shields, a GPS shield was used to identify the pond being sampled. For communication, a Dragino LoRa [31] shield was used to stream DO and temperature sensor data to the server in the farm manager's office. The LoRa antenna was mounted on a pole at the back of the truck (Figure 5a).

The system was deployed on Logan Hollow Farm between September and October 2019. Logan Hollow Fish Farm is located in southwest Illinois in the bottomland of the Mississippi River. This is a comparatively small farm with 70 ponds. For DO monitoring, the farm employed two technicians to drive the trucks and sample each pond during the night. A total of 15 days of data were collected using the automated system on the farm during this period. The systems were again deployed at another collaborating farm-Flowers Fish Farm, in the summer of 2021 to collect additional data.

These datasets are critical to improving the prediction model. The model development effort will be presented in future work. More importantly, these deployments helped us gain our farm collaborators' trust.

As evidence of the success of the system deployment in reducing the barriers to the acceptance of robotic technology by the fish farmers, Mr. Pete Reiff, Logan Hollow's Owner/Operator, requested the HBOI sensing system to be installed on the second truck of his farm [32]. One immediate tangible benefit that the farm can gain from the automated system is to allow the farm to collect high-quality DO data consistently. The current

paper-based operation is crude and fraught with potential decision-making problems (e.g., transcription issues of the data collected), as shown in Figure 6.



(**a**)

(**b**)

Figure 6. Hand-written sheets of DO data collected on the Logan Hollow farm by different farm technicians. The quality of the sheet ranges from good in (**a**) "good" quality DO datasheet to almost illegible in (**b**) "bad" quality DO datasheet.

3. Development and Field Demonstration of Drone-Based HAUCS Sensing Payload

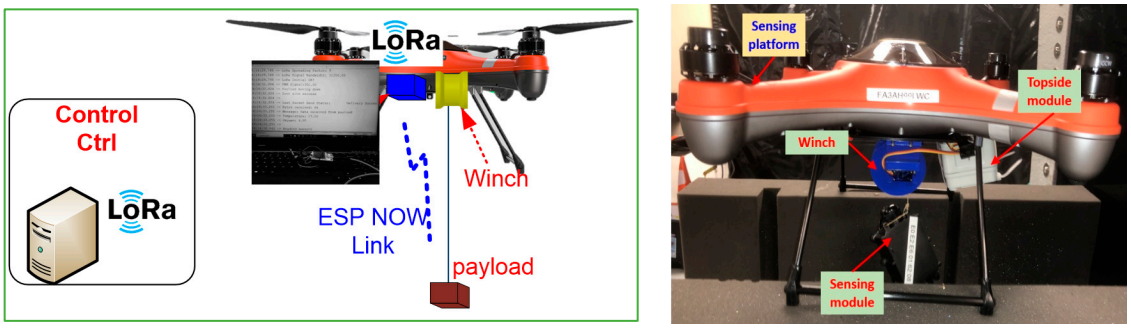
3.1. Development of Drone-Based HAUCS Sensing

For this effort, a low-cost Swellpro Splashdrone 3+ was adopted for payload integration (https://www.swellpro.com/waterproof-splash-drone.html, accessed on 11 March 2021). Splashdrone™ is a waterproof drone that is surface buoyant. The Splashdrone 3+ employs the conventional quadcopter design, sports an axis diameter of 450 mm, a flight time of 20–23 min, a weight of 2 kg, and a max payload capacity of 1 kg. Such payload capability is ideal for HAUCS platforms. Another important consideration is that this drone can operate in heavy rain with winds up to 18 mph and gusts of up to 31 mph. In addition, the vendor will provide API to support the integration of external logic with the drone in the near future. The programming capability will be desirable for the future implementation of environmental adaptive path planning algorithms [33]. However, one important insight the team arrived at in designing for the project is that instead of being locked into specific platform designs, the HAUCS sensing payload should be platform-neutral. Therefore, while the new sensing payload targets an aerial drone, it can be easily adapted to other platforms, such as unmanned surface vehicles (USVs) or ground vehicles.

The sensing system has two subsystems: a payload module containing the sensors and microcontroller to support data acquisition and transmission to the topside module and a topside module that interfaces with the platform (aerial drone in this case) forward data to the control center via a long-range communication link. The two modules are connected with a winch that will be released to allow the sensors to go underwater during the sensing operations (Figure 7).

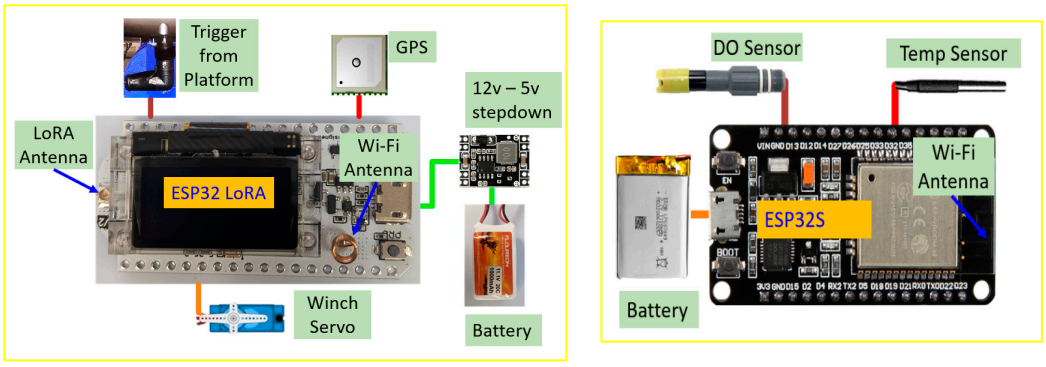
The topside is the gateway between the sensing module and the control center. The topside engages the winch to release and retrieve the sensing module during the sensing operation. The engagement can be triggered by signals from the sensing platform (which is the current implementation) or by GPS-driven waypoint programming (i.e., positioned over a pond and at proper altitude). To perform these tasks, the topside module contains a micro-controller, a GPS unit, and a servo that controls the winch (Figure 8a). A LoRA link is adopted to support the communication between the sensing platform and the control center [30]. However, other options may also be considered. For example, the SIYI 2.4 G Datalink can support video links up to 15 km range, albeit at increased weight and power than LoRA links [34]. To support the LoRA link, the ESP32 LoRA controller is

ideal due to its rich connectivity options: LoRA, WiFi, and Bluetooth [35]. The payload module handles the sensor data acquisitions and quality control (QC). Temperature and DO sensors are included in the module. Here, the controller is an ESP32S [36], which consumes less power than ESP32 LoRA while supporting multiple analog to digital converter (ADC) channels and WiFi links. The communications between the topside and the sensing modules are achieved using the ESP-NOW link [37]. ESP-NOW is a connectionless communication protocol developed by Espressif to support short packet transmission (up to 250 bytes) between ESP32 boards. This protocol enables multiple devices to talk to each other using the 2.4GHz RF circuits on the ESP32x boards without the WiFi protocol. Therefore, this protocol is ideal for linking topside and sensing modules. The lightweight ESP-NOW link helps eliminate the need for a physical electrical connection between topside and sensing modules and simplifies the winch system. As a result, the winch essentially consists of a servo that controls the release and retrial of the sensing module using a metal chain (Figure 9).



(**a**) (**b**)

Figure 7. Illustration of the platform-independent sensing system design. (**a**) A flow chart describes the components in the sensing system. The sensor data will be sent via the ESP ONE wireless link from the topside module. The topside will relay the data to the control center via long-range communication links such as LoRa. (**b**) Showing the integration of the sensing system with the Splashdrone.



(**a**) (**b**)

Figure 8. Flow charts describe the topside and payload modules. (**a**) The flow chart illustrates the topside electronic. (**b**) A flow chart shows the sensing module electronic.

The drone will be programmed to reach a pre-defined location over the pond and transition to hovering mode during the sensing operation. Once the drone is on location, the sensing module release will be triggered (either via a signal from the sensing platform or a pre-determined waypoint). The topside will, in turn, engage the winch to lower the payload module into the water. The payload module loses communication with the topside module when fully submerged in water. The payload module will start acquiring DO and temperature data for a pre-determined time (i.e., 20 s) and store the data onboard the controller. The topside will then retrieve the winch after the data acquisition period. Once the payload module is fully retrieved, the data stored on the payload module controller

will be sent via the ESP-NOW link to the topside. The repackaged data (i.e., adding the GPS coordinates and timestamps) will be forwarded to the control center for processing.

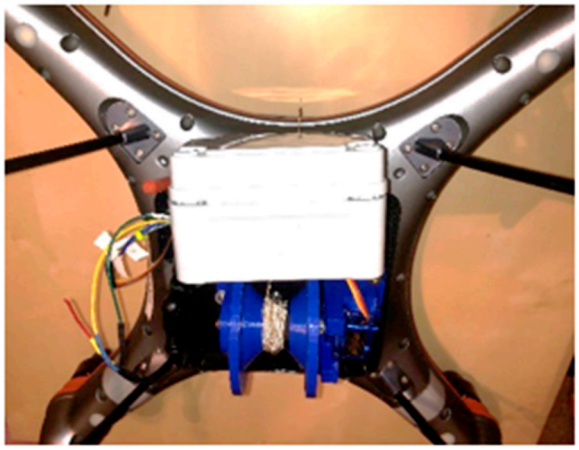


Figure 9. Winch to release/retrieve the sensing module.

While drones are the primary platform, the platform-neutral nature of the sensing system design ensures that the payload is compatible with other platforms such as all-terrain vehicles (ATVs) or unmanned surface vehicles (USVs).

3.2. Lab and Field Deployment

The initial test was a static test inside the System and Imaging Laboratory (SAIL) lab. During the test, the payload is mounted on the drone. However, the drone was fixed to the lab ceiling and kept idle. A trigger signal was sent from the drone transmitter to the drone during the test. The signal triggered the sensing operation: the topside module engaged the winch to release the payload; the payload then idled for 20 s to simulate the data acquisition period; the topside retrieved the payload (Figure 10). All these were done in an automated fashion. The communication links from the sensing module to the topside (through ESP-NOW) and from the topside to the control center (via LoRA) were validated.

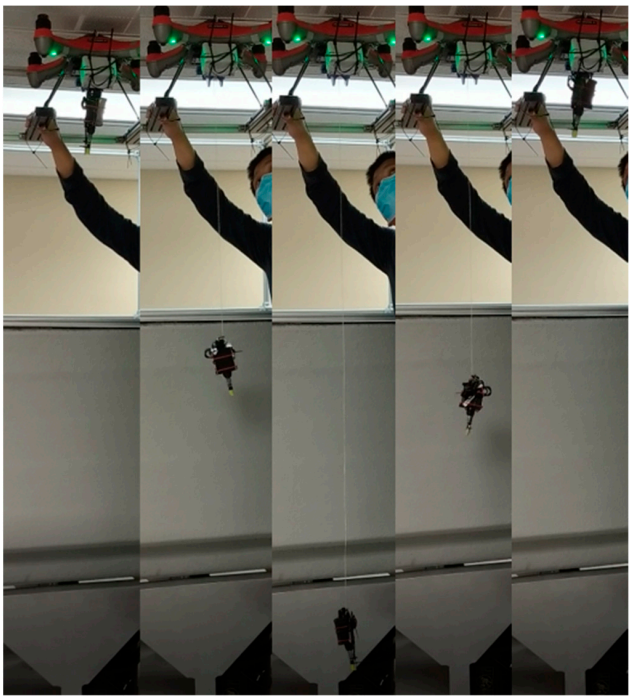


Figure 10. Lab test for the payload release and retrieve.

Following the lab test, the system was further tested over the ground at the HBOI campus to validate the feasibility of the sensing operation. Here, the objective was to deploy the payload into a plastic tub with a 1.5 m diameter. Video frames that illustrate the whole process are in Figure 11.

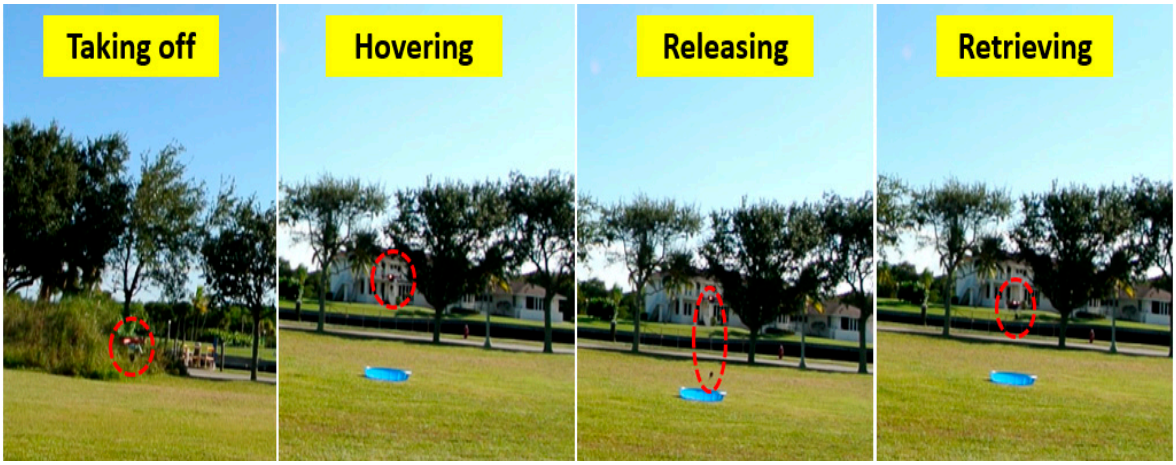


Figure 11. Field validation of the sensing operation.

The system was set up at our research collaborator Flowers Fish Farm in October 2021 for the initial field test of the drone-based sensing operation. With the consent of the farm owner, Ms. Kelly, and manager, Mr. Frampton, the HBOI team (Dr. Paul S. Wills) piloted the drone during the tests (Figure 12).



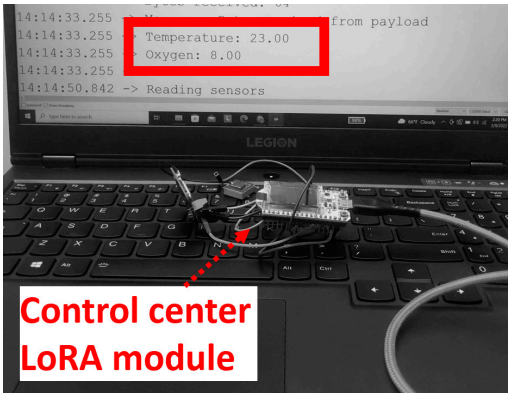
(**a**) (**b**)

Figure 12. (**a**) Photos were taken during the preparation of the field test at Flowers Fish Farm. From left to right: Ms. Kelly Flowers, the Flowers Fish Farm owner. Mr. Mike Frampton, Farm Manager, and Dr. Paul Wills. (**b**) The Splashdrone integrated with the sensing system during the flight at Flowers Fish Farm in Dexter, MO.

Since the primary goal of the experiment was to validate the functionalities of the sensing system and identify any potential issues, the tests were conducted during the daytime when the farmworkers were present. During the tests, Dr. Wills acted as the pilot to command the drone takeoff and landing, and flew the drone to the desired location in the pond for a simulated sensing operation (Figure 13a).



(**a**)



(**b**)

Figure 13. (**a**) Frames from the video clip taken during the field test to validate the functionality of the drone-based sensing system. The frames illustrate the drone taking off, deploying payload, retrieving the payload, and flying back to base. (**b**) Photo shows the sensor data acquired during the test received at a laptop equipped with a LoRA module at the control center.

While the field tests validated the basic concept, one issue we identified during the tests was that since the payload was connected to the drone body with a string, it is more susceptible to ambient environmental conditions. For example, strong side wind could induce a pendulum effect on the payload, impacting the drone's flight stability.

To address this issue, we aim to develop a deployable robotic extension that can provide better controllability and expand the functionality of the sensing payload. In this regard, we are exploring an Origami-based robotic extension. We will discuss the initial feasibility study of the Kresling Kirigami drone robotic extension design through both CAD modeling and laboratory testing. A more focused study of the Kresling Kimigami robotic extension will be presented in a future manuscript.

4. Feasibility Study of a Kresling Kirigami Robotic Extension Design

The design choice is motivated by several factors. First, the robotic extension for the HAUCS will need the flexibility of support with varying extension lengths. Secondly,

the folding and unfolding should be confined to the same horizontal footprint to avoid interference with other sensors to be integrated into the drone, such as cameras and other environmental sensors. Thirdly, the actuation needs to be supported via the drone flight controller. For this reason, we investigated a Kresling buckling pattern-based design.

Furthermore, in our implementation, we opted for Kirigami instead of Origami. In addition to folding, Kirigami also involves cutting. There are more than simple semantic differences between Kirigami and Origami. For example, Li et al. adopted Kirigami enhancement to prevent wrinkling during continuous folding/unfolding and improve structure reliability [15]. Yasuda uses a similar methodology where he makes small, precise cuts and inserts small holes in areas where continual stresses may lead to creasing and deformation in the mesh [38]. Many others use Kirigami to construct self-folding structures [39,40]. For the HAUCS robotic extension, we also envision the need for continuous folding/unfolding during the sensing operations. This, therefore, motivated us to adopt a Kirigami-based design.

4.1. Kresling Kirigami Prototype Design

The proposed robotic extension consists of multiple Kresling Kirigami sections. Each section consists of two plates connected with hinges (i.e., Kirigami creases). The torsional loading is realized via the plate rotating at the center axis, driven by a gear system at one end and a ball bearing at the other. The hinges then rotate in conjunction with the rotation of the main body, allowing the structure to fold and unfold. The gear and bearing will be mounted on a set of collapsible tapered rods.

A Solidworks model of this design was developed to support laboratory evaluations. In the prototype design, the full extension of one Kirigami section is 82.8 mm, and a folded section has a height of 20.2 mm. The diameter of the structure is 85 mm (Figure 14).

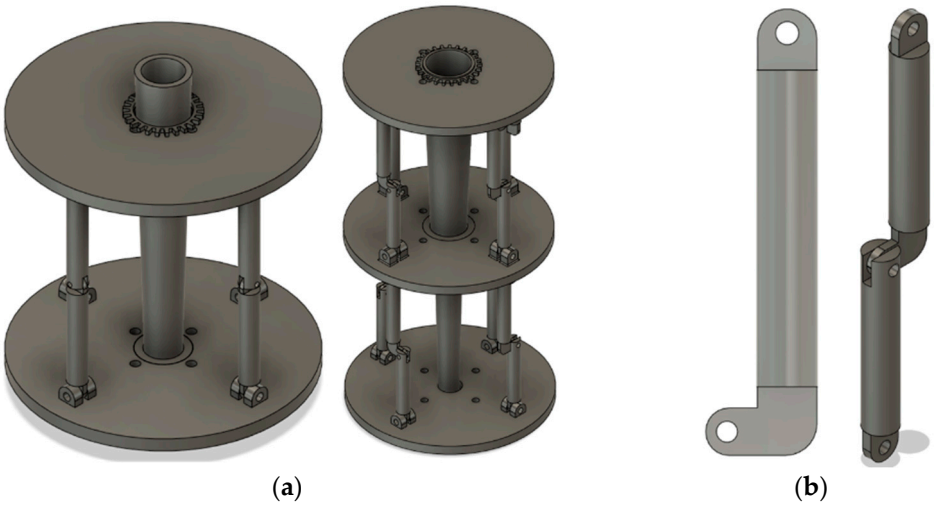


Figure 14. The three images from left to right show the folding of a single Kirigami section.

The central axis is a telescopic rod that can collapse in the current design. The structure is composed of multiple Kirigami sections. Each Kresling Kirigami section can collapse independently to realize a variable-length robotic extension (Figure 15a).

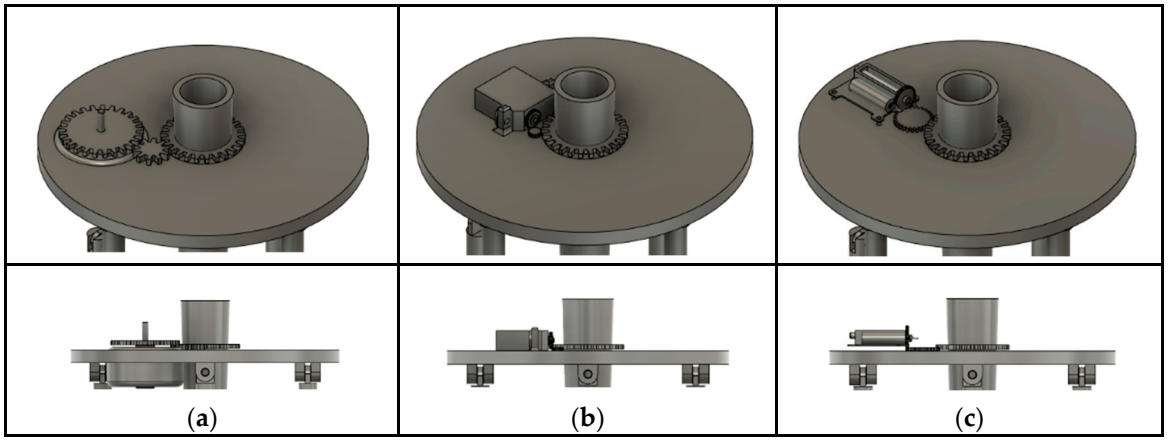
One key component in supporting the structure folding and unfolding is the uniquely designed hinge. This Kirigami design requires each hinge to rotate 180 degrees. An action that is not supported by traditional straight hinge pins. Instead, the devised hinge pin sports an 'L' shaped attachment joint (Figure 15b). This hinge design accomplishes two essential requirements. The first, as previously mentioned, is the ability to rotate 180 degrees. The second is a locker system on one side to maintain rigidity, and compression only occurs in one direction.

Another critical design consideration is to use a gear system to realize the torsional loading. The gear system can be driven by a servo, worm drive, or stepper motor (Figure 16), With this design, each Kirigami section can be actuated independently from the drone flight controller (Figure 16).



(**a**) (**b**)

Figure 15. (**a**) The CAD models of a single section and two-section Kresling Kirigami incorporate gear-driven actuation. (**b**) The 'L' shaped hinges support 180-degree rotation.



(**a**) (**b**) (**c**)

Figure 16. Three different actuation options to drive the utilizing: (**a**) a step motor, (**b**) micro servo, and (**c**) a linear actuator.

4.2. Laboratory Validations

Small-scale models were constructed and subjected to dynamic force to determine efficacy. During the CAD modeling, "mockups" were first created by utilizing the most simplistic materials, foam board, and bendable straws to provide physical proof of concept. Once CAD models were established, the components were printed on 3D printers and assembled. Figure 17 illustrates the folding of a sing-section structure and a two-section structure. Figure 17a–c illustrates the single-section structure begins in the locked position, with hinges at full extension. Through manual actuation, the structure compresses along the *z*-axis until it is fully folded. The same process is conducted for a two-section unit shown in Figure 17d–g.

Load tests were performed on the single unit model. The tests were conducted by adding water to various containers placed on top of the unit. This test determined that the model would suffer structural failure at 1802 g of applied weight (Table 1). The test measured structural integrity to the applied load. A green indicator value was given when the structure maintained its integrity with little to no deflection, similar to the elastic region. Yellow was given when the structure exhibited signs of deflection consistent with the plastic region. Red was given for the point of failure or fracture. Figure 18 illustrates the corresponding behavior of the structure under different loads.

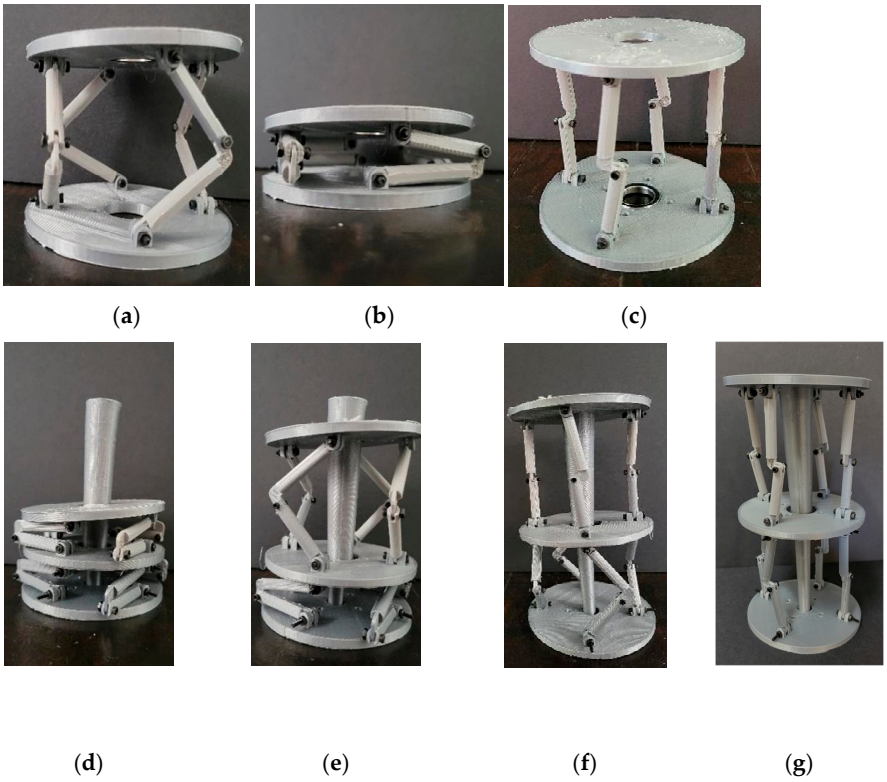


Figure 17. Revolute body frame in expansionsequence, in both single unit (**a**–**c**) and double-stacked arrangements (**d**–**g**).

Table 1. Results of load failure test of a single-section structure. Structure support denotes any deformations suffered during loading: green means little to no deformation, yellow is significant deformation, and red marks the point of failure.

Weight (g)	401	550	700	1512	1605	1727	1802
Structure							



Figure 18. Weight of load applied to the revolute structure and resulting structural deformations. The photos in the top row show the actual load and those in the bottom row show the responses to the structure deformations.

Similar tests were conducted against a two-section structure. Here, two different cases were evaluated. In the first case, the top section was initially fully extended. The results are summarized in Table 2 and the actual deformations are illustrated in Figure 19. Here, the top section experienced failure at a lower loading than the bottom layer, which behaved similarly to the single-section case.

Table 2. Results of load failure test of a two-section structure. The structural support is ranked the same as Table 1, with only two points of failure as there are two individual units.

Weight (g)	401	701	1000	1251	1654	1800	1900	2050
Structure 1								
Structure 2								



Figure 19. Weight of load applied to a fully extended two-section structure.

Further investigation may be needed to explain the cause fully. Still, one likely reason was the misalignment between the two sections—the parts were printed in a low-quality setting to support rapid prototyping. In the second test, the top section was half folded. As results in Table 3 and Figure 20 show, the behavior of the bottom section is similar to that of a single section as expected. However, the top section was able to withstand less loading. We did not integrate any electronic actuator into the prototype.

Table 3. Results of load failure test of a fully extended two-section structure with the top section half folded initially.

Weight (g)	18	100	306	506	1350	1852	1900
Structure 1							
Structure 2							

Upon completion of these experiments, the model was examined. While the prototype was structurally weakened from the collapse, it was not irreparably damaged. The prototype was still able to fold and unfold properly. The prototype could also withstand axial loading, although with decidedly lighter weights than previously observed.

The next step in laboratory testing will be to evaluate the actuation, in particular, comparing the effectiveness of step motor, micro servo, and worm drive to actuate the Kirigami structure through the gear system. This is a critical and necessary step before

further mechanical design optimizations. Unfortunately, we are hindered by the short supply of the electronic components needed for this work. However, we intend to provide a thorough study of the Kirigami robotic extension design in a separate manuscript.



Figure 20. Weight of load applied to a two-section structure with the top section half folded initially.

5. Conclusions

A significant expense in most pond aquaculture farm operations is the labor and vehicle fuel cost related to the DO sensing practice. The overarching goal of the HAUCS framework is a transformative robotic solution for aquaculture farms of varying scales to achieve collaborative monitoring and decision-making. Once fully developed, the HAUCS sensing platform can overcome the shortcomings in many existing aquaculture farm monitoring solutions such as the static pond buoy type sensors. These sensors may face the challenges of being susceptible to biofouling, high deployment costs, and maintenance difficulty.

An essential aspect of our work is the experience we gained on how to move forward in any field of robotic development in an industry that is generally risk-averse regarding new technology due to the high cost for initial adopters and the low profit margins such as the aquaculture farms. As we realized from early on, one of the most critical components of the HAUCS project is the close engagement with the farms and buying-in from the farmers. In this regard, the team achieved great success, demonstrated by the support from our collaborative farms throughout the development and testing of HAUCS infrastructure and platforms. Our success in this aspect can benefit many similar field robotic projects.

One of the crucial achievements in technology development is the HAUCS AUP—the mobile environmental sensing system. The successful deployment of the prototype system on an operational fish farm validated the effectiveness of the design and will be the foundation to build upon for future efforts. It is worth noting that our work is the first known attempt at drone-based mobile DO monitoring system for the aquaculture farm setting. The HAUCS system is a transformative technology that can revolutionize how pond aquaculture farms operate. In addition to significant savings in labor and time through the automation of the DO monitoring of the ponds on the farm, HAUCS can provide unprecedented insight into the spatial variations of each pond that none of the existing state-of-the-art techniques are

capable of. At the same time, the HAUCS system avoids many drawbacks that plague these techniques, such as biofouling and maintenance difficulties.

While the initial motivation for developing the Kirigami-based robotic extension is to improve the drone's stability during the sensing operation, this extension can significantly enhance the AUP's functionalities, such as supporting/stabilizing underwater cameras or sonars or collecting water samples. These capabilities will help expand the HAUCS framework's applicability to support other environmental monitoring efforts, such as surveillance of coastal zone harmful algae bloom (HAB) [41]. While this development is still in the early stages, the laboratory tests of the mechanical models verified that the design is sound.

It is worth noting that while the primary objective is to support drone-based sensing, one unique aspect of the system is that it is platform-neutral. As a result, the system can be easily adapted to other platforms, such as unmanned surface vehicles (USV).

Going forward, one main focus of the project will be the operational deployment of the HAUCS framework. Here, multiple HAUCS platforms will be deployed on our collaborative farms to conduct farm environmental monitoring to complement the current DO sensing practices during farm operations. In addition to improving the reliability and reducing the power consumption of the sensor payload, one critical component to support such deployment is implementing the hybrid path planning algorithm [33] in the HAUCS framework.

The initial modeling of the Kirigami-based robotic extension validated the basic design concept. With further development, the Kirigami-based extension will be able to perform the desired HAUCS tasks. It can be adapted for more advanced operations (e.g., attaching a gripper or tube for physical collection). Going forward, several topics need to be further explored. Different drive options to actuate the Kirigami structure (i.e., servo, worm drive, and step motor) will be investigated through laboratory experiments to test the integration with the drone flight controller while avoiding a significant weight increase. The mechanical design will be further improved to reduce the volume of the structure in the compressed form. Following the same trajectory of our payload development, we aim to integrate the robotic extension with the drone and field test in the implementation on the collaborative farm.

6. Patents

Bing Ouyang, Paul Wills, Casey Den Ouden and Lucas Lopes, "Platform-Independent Mobile Environmental Sensing System," US Patent Application 63/311,937, 02/18/2022.

This invention was made with government support under Contract No. 2019-67022-29204, awarded by the National Institute of Food and Agriculture/United States Department of Agriculture.

Author Contributions: Conceptualization, B.O., P.S.W. and C.J.D.O.; methodology, C.J.D.O., B.O. and P.S.W.; software, L.L.; validation, P.S.W., B.O., L.L. and J.S.; resources, B.O. and P.S.W.; data curation, C.J.D.O.; Kirigami design and testing, C.J.D.O.; writing—original draft preparation, C.J.D.O., B.O., L.L., P.S.W. and J.S.; writing—review and editing, C.J.D.O. and B.O.; visualization, C.J.D.O.; supervision, B.O.; funding acquisition, B.O. and P.S.W. All authors have read and agreed to the published version of the manuscript.

Funding: This research was funded with support under Contract No. 2019-67022-29204, awarded by the National Institute of Food and Agriculture/United States Department of Agriculture.

Acknowledgments: The authors want to thank Yanjun Li and Dennis Estrada for helping during the laboratory tests. Ben Metzger for the discussions on the mechanical design of the Kirigami structure.

Conflicts of Interest: The authors declare no conflict of interest. The funders had no role in the design of the study, in the collection, analyses, or interpretation of data, in the writing of the manuscript, or in the decision to publish the results.

References

1. Aravind, K.R.; Raja, P.; Pérez-Ruiz, M. Task-based agricultural mobile robots in arable farming: A review. *Span. J. Agric. Res.* **2017**, *15*, e02R01. [CrossRef]
2. Bhandari, S.; Raheja, A.; Green, R.L.; Do, D. Towards collaboration between unmanned aerial and ground vehicles for precision agriculture. In *Autonomous Air and Ground Sensing Systems for Agricultural Optimization and Phenotyping II*; SPIE: Orlando, FL, USA, 2017; Volume 10218.
3. Schimmelpfennig, D. Precision Agriculture Technologies and Factors Affecting Their Adoption. 12 May 2016. Available online: https://www.ers.usda.gov/amber-waves/2016/december/precision-agriculture-technologies-and-factors-affecting-their-adoption/ (accessed on 1 February 2018).
4. Meola, A. IOT-101: The Essential Guide to the Internet of Things. April 2018. Available online: https://artillry.co/wp-content/uploads/2019/08/Business-Insider-IOT-101.pdf (accessed on 11 August 2020).
5. *The State of World Fisheries and Aquaculture 2020*; Food and Agriculture Organization of the United Nations: Rome, Italy, 2020.
6. What Is Aquaculture and Why Do We Need It? *Global Aquaculture Alliance.* Available online: https://www.aquaculturealliance.org/blog/what-is-aquaculture-why-do-we-need-it/ (accessed on 24 November 2020).
7. Yuan, Q.; Song, G.; Fullana-I-Palmer, P.; Semakula, H.; Mekonnen, M.; Zhang, S. Water footprint of feed required by farmed fish in China based on a Monte Carlo-supported von Bertalanffy growth model: A policy implication. *J. Clean. Prod.* **2017**, *153*, 41–50. [CrossRef]
8. Hall, S.; Delaporte, A.; Phillips, M.; Beveridge, M.; O'Keefe, M. *Blue Frontiers: Managing the Environmental Costs of Aquaculture*; The WorldFish Center: Penang, Malaysia, 2011.
9. Aquaculture Production (Indicator). OECD. 2020. Available online: https://doi.org/10.1787/d00923d8-en (accessed on 24 November 2020).
10. Dureisseix, D. An Overview of Mechanisms and Patterns with Origami. *Int. J. Space Struct.* **2012**, *27*, 1–14. [CrossRef]
11. Lang, R.J. Origami: Complexity increases (again). *Eng. Sci.* **2004**, *67*, 5–19.
12. Zirbel, S.; Magleby, S.; Howell, L.; Lang, R.; Thomson, M. Accommodating thickness in origami-based deployable arrays. *J. Mech. Des.* **2013**, *135*, 111005. [CrossRef]
13. Li, Y.; Liu, W.; Deng, Y.; Hong, W.; Yu, H. Miura-ori enabled stretchable circuit boards. *Nat. Partn. J.-Flex. Electron.* **2021**, *5*, 1–9. [CrossRef]
14. Thrall, A.P.; Quaglia, C.P. Accordion shelters: A historical review of origami-like deployable shelters developed by the US military. *Eng. Struct.* **2013**, *59*, 686–692. [CrossRef]
15. Randall, C.L.; Gultepe, E.; Gracias, D.H. Self-folding devices and materials for biomedical applications. *Trends Biotechnol.* **2012**, *30*, 138–146. [CrossRef]
16. Peraza-Hernandez, E.A.; Hartl, D.J.; Malak, R.J., Jr.; Lagoudas, D.C. Origami-inspired active structures: A synthesis and review. *Smart Mater. Struct.* **2014**, *23*, 094001. [CrossRef]
17. Kresling, B. Plant Design: Mechanical Simulations of Growth Patterns and Bionics. *Biomimetics* **1995**, *3*, 105–222.
18. Guest, S.D.; Pellegrino, S. The Folding of Triangulated Cylinders Part I: Geometric Considerations. *ASME J. Appl. Mech.* **1994**, *61*, 773–777. [CrossRef]
19. Guest, S.D.; Pellegrino, S. The Folding of Triangulated Cylinders Part II: The Folding Process. *ASME J. Appl. Mech.* **1994**, *61*, 778–783. [CrossRef]
20. Guest, S.D.; Pellegrino, S. The Folding of Triangulated Cylinders Part III: Experiments. *ASME J. Appl. Mech.* **1996**, *63*, 77–83. [CrossRef]
21. Kresling, B. Folded Tubes as Compared to Kikko ("Tortoiseshell") Bamboo. In *Origami*; AK Peters: Natick, MA, USA, 2001; pp. 197–207.
22. Hunt, G.W.; Ario, I. Twist buckling and the foldable cylinder: An exercise in origami. *Int. J. Non-Linear Mech.* **2005**, *40*, 833–843. [CrossRef]
23. Nishiyama, Y. Miura Folding: Applying Origami to Space Exploration. *Int. J. Pure Appl. Math.* **2012**, *79*, 269–279.
24. Yoshimura, Y. *On the Mechanism of Buckling of a Circular Cylindrical Shell under Axial Compression*; NACA: Washington, DC, USA, 1955.
25. Kresling, B. Origami-structures in natures: Lessons in designing 'smart' materials. In *Symposium OO—Multiscale Mechanics of Hierarchical Materials*; Cambridge University Press: Cambridge, UK, 2012.
26. Kim, S.J.; Lee, D.Y.; Jung, G.P.; Cho, K.J. An origami-inspired, self-locking robotic arm that can be folded flat. *Sci. Robot.* **2018**, *3*, 1–10. [CrossRef]
27. Miura, K.; Tachi, T. Synthesis of rigid-foldable cylindrical polyhedra. In Gmuend, Austria. *Symmetry Art Sci.* **2010**, 204–213.
28. Ouyang, B.; Wills, P.S.; Tang, Y.; Hallstrom, J.O.; Su, T.C.; Namuduri, K.; Mukherjee, S.; Rodriguez-Labra, J.I.; Li, Y.; Ouden, C.J. Initial Development of the Hybrid Aerial Underwater Robotic System (HAUCS): Internet of Things (IoT) for Aquaculture Farms. *IEEE Internet Things J.* **2021**, *8*, 14013–14027. [CrossRef]
29. LoRa Alliance. A technical overview of LoRa®and LoRaWAN™. May 2015. Available online: https://lora-alliance.org/sites/default/files/2018-04/what-is-lorawan.pdf (accessed on 25 June 2018).

30. Ouyang, B.; Wills, S.P.; Li, Y.; den Ouden, C. Hybrid Aerial Underwater Robotic System (HAUCS): The Initial Instruments Development and Deployment. In Proceedings of the 2020 IEEE 92nd Vehicular Technology Conference (VTC2020-Fall), Victoria, BC, Canada, 18 November–16 December 2020.
31. SIYI. 2.4G Datalink User Manual. Available online: https://discuss.ardupilot.org/uploads/short-url/sgfUtaqa7P5KZ8r4jRcTUtVpzoW.pdf (accessed on 9 July 2021).
32. Heltec. WiFi LoRa 32 (V2). Available online: https://resource.heltec.cn/download/WiFi_LoRa_32/WIFI_LoRa_32_V2.pdf (accessed on 5 April 2021).
33. Shenzhen Anxinke Technology. ESP-32SDatasheet. 3 October 2016. Available online: https://www.es.co.th/Schemetic/PDF/ESP32.PDF (accessed on 1 June 2021).
34. espressif. ESP-NOW. Available online: https://docs.espressif.com/projects/esp-idf/en/latest/esp32/api-reference/network/esp_now.html (accessed on 1 June 2021).
35. Van Manen, T.; Janbaz, S.; Ganjian, M.; Zadpoor, A.A. Kirigami-enabled self-folding origami. *Mater. Today* **2020**, *32*, 59–67. [CrossRef]
36. Reid, A.; Lechenault, F.; Rica, S.; Adda-Bedia, M. Geometry and design of origami bellows with tunable response. *Phys. Rev. E* **2016**, *95*, 013002. [CrossRef]
37. Saito, K.; Tsukahara, A.; Okabe, Y. Designing of self-deploying origami structures using geometrically misaligned crease patterns. *R. Soc.* **2016**, *472*, 20150235. [CrossRef] [PubMed]
38. Sellner, K.G.; Doucette, G.J.; Kirkpatrick, G.J. Harmful algal blooms: Causes, impacts and detection. *J. Ind. Microbiol. Biotechnol.* **2003**, *30*, 383–406. [CrossRef] [PubMed]
39. Mukherjee, S.; Ouyang, B.; Kamesh, N.; Wills, P.S. Multi-Agent Systems (MAS) related data analytics in the Hybrid Aerial Underwater Robotic System (HAUCS). In *Big Data III: Learning, Analytics, and Applications*; SPIE: Washington, DC, USA, 2021; Volume 11730.
40. Kresling, B. Natural twist buckling in shells: From the hawkmoth's bellows to the deployable Kresling-pattern and cylindrical Miura-ori. In Proceedings of the 6th International Conference on Computation of Shell and Spatial Structures, Ithaca, NY, USA, 28–31 May 2008.
41. Srinvasan, A. *Handbook of Precision Agriculture: Principles and Applications*; CRC Press: Boca Raton, FL, USA, 2006.